ELSEVIER

Journal of Structural Geology 27 (2005) 357–370

JOURNAL OF STRUCTURAL GEOLOGY

www.elsevier.com/locate/jsg

# Textures recording transient porosity in synkinematic quartz veins, South Coast, New South Wales, Australia

John V. Smith*

*Natural Resource Engineering Discipline, School of Civil and Chemical Engineering, RMIT University, GPO Box 2476V, Melbourne 3001, Victoria, Australia*

Received 3 February 2003; received in revised form 19 March 2004; accepted 26 September 2004
Available online 2 December 2004

**Abstract**

The textures of synkinematic veins involve a complex interplay of crystal growth and deformation. Quartz veins in Devonian sandstone and altered felsic volcanic rocks of the South Coast region of New South Wales, Australia, display a range of microstructures recording complex vein growth mechanisms. The synkinematic veins have not suffered significant later imposed deformation and all deformational features within the veins are associated with the kinematics of vein formation. The veins are commonly fibrous but growth patterns are not restricted to simple margin-parallel types (for example, antitaxial and syntaxial). Mineral fibres and blocky cavity fillings developed concurrently throughout all stages of vein growth. Dilation and pressure-solution of vein textures is recorded by transgranular, intergranular, and intragranular deformation microstructures. Textures of progressively deformed synkinematic veins, such as arrays of sigmoidal vein and shear veins related to folding, contain microscopic folds and faults of fibrous quartz and the development of crystallographically controlled microcrack arrays within crystals. Small displacements of the microcrack arrays locally rotate the crystal lattice and at low power magnification are indistinguishable from non-brittle shear bands. Where arrays of veins have been linked to form through-going fault veins, intense deformation microstructures combine with a variety of cavity growth features including dilation of weaknesses such as micaceous seams.


*Keywords:* Textures; Porosity; Synkinematic; Quartz veins; Deformation

## 1. Introduction

Vein textures can be interpreted in terms of features recording vein opening and features recording later deformation of the vein-filling minerals. In synkinematic veins there is potential for both these textural types to occur together as a vein filling evolves. Durney and Ramsay (1973) emphasized the synkinematic nature of many veins, filled by elongate or fibrous minerals, and introduced an interpretation of veins which focused on margin-parallel growth sites, namely: vein centres (syntaxial), vein margins (antitaxial), combinations of these types (composite) and randomly located margin-parallel fractures ('stretched' crystals). In their model, en échelon arrays of fractures open and propagate progressively within the bulk kinematics of a dilatant shear zone. Sigmoidal shapes develop as the central part of each vein progressively rotates whilst the fracture propagation direction remains steady. An alternative explanation for sigmoidal veins is the bending of rock bridges between adjacent fracture segments such that the inner margins of the fractures become curved (Nicholson and Pollard, 1985). Smith (1999) interpreted the latter process to be more representative of the formation of arrays of sigmoidal quartz veins exposed on the south coast of New South Wales, Australia, based on morphological characteristics. Nevertheless in both mechanisms, the progressive deformation responsible for the sigmoidal shape of veins can potentially deform the vein-filling minerals and textures.

Antitaxial vein growth can be localized along one margin of a vein as evidenced by unidirectional textural trends such as coarsening and changes in spacing between individual inclusions in wall rock trails and a progression from fibrous grains to blocky euhedrally terminated grains (Fisher and

* Tel.: +61-3-9925-2208; fax: +61-3-9639-0138
*E-mail address:* johnv.smith@rmit.edu.au.

0191-8141/$ - see front matter © 2004 Elsevier Ltd. All rights reserved.
doi:10.1016/j.jsg.2004.09.003

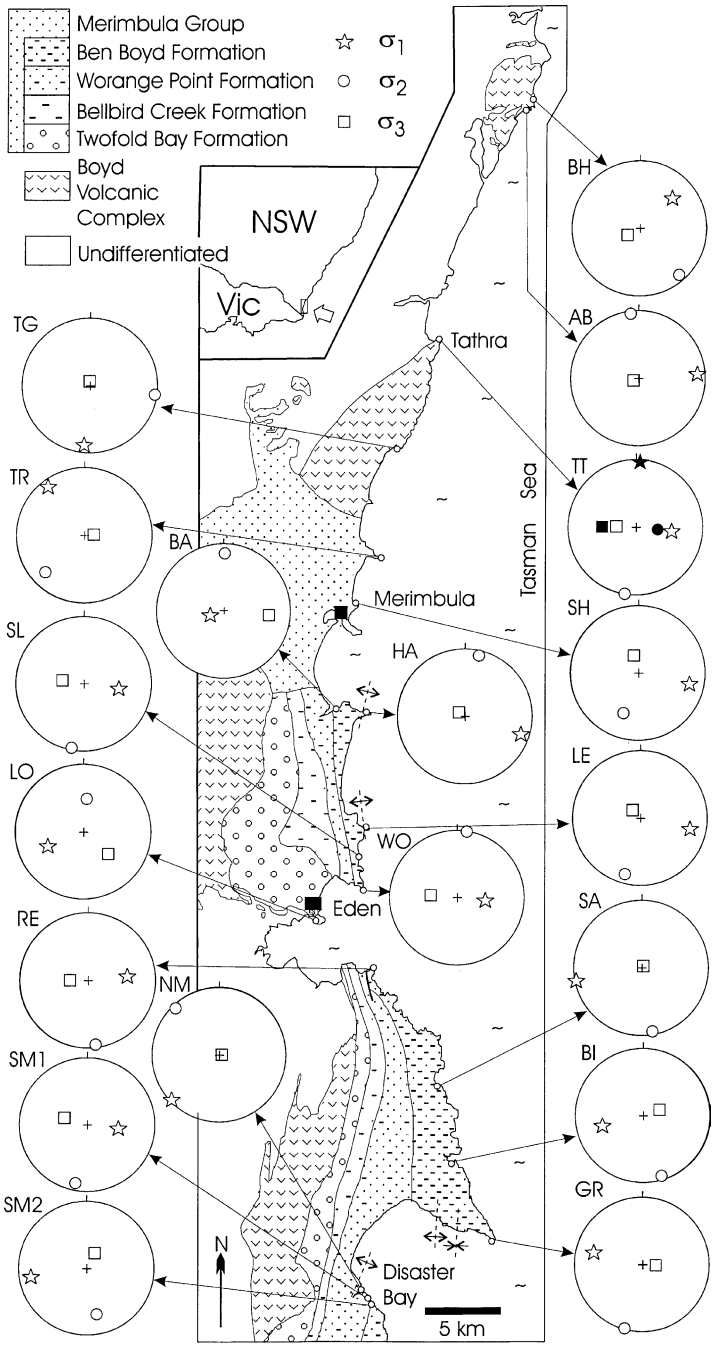


Fig. 1. Location and geological maps (modified from Lewis et al. (1994)). Stereographs (equal angle) show the orientation of principal stress axes (subscript 1 is maximum compression) inferred from quartz vein arrays sampled and investigated in this study. Localities from north to south are: Bunga Head (BH), Aragunnu Bay (AB), Tathra Head (TT, open and bold symbols represent determinations from two adjacent vein arrays), Turingal Head (TG), Tura Head (TR), Short Point (SH), Barmouth, Pambula (BA), Haycock Point (HA), Lennards Island (LE), South of Lennards Island (SL), Worange Point (WO), Lookout Point (LO), Red Point (RE), Saltwater Creek (SA), Bitangabee Bay (BI), Green Cape (GR), North of Merrica River (NM), South of Merrica River 1 (SM1), South of Merrica River 2 (SM2). Grid references available from author on request.

Brantley, 1992; Brantley et al., 1997). For antitaxial growth, the solute can be envisaged to travel through the host-rock matrix to the vein margin either by grain-boundary diffusion (Durney and Ramsay, 1973) or flow of solution through micropores (Means and Li, 2001). In the case of veins with internal growth sites (syntaxial, composite and 'stretched' crystals) the mineral solutes must somehow gain access to the inner parts of the vein. For interconnected vein systems, fluid flow through a fracture network can be inferred (e.g. Cox, 1999). However, for isolated veins (such as in en échelon arrays) internal growth mechanisms require pathways for permeability or diffusion (Gray et al., 1991) through the deposited mineral phase to link the growth sites with the surrounding host-rock.

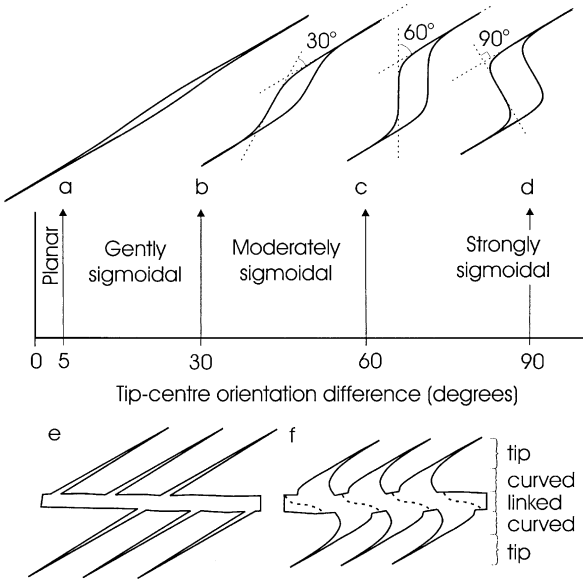


Fig. 2. (a)–(d) Definition of terminology for geometric en échelon vein types. (e) and (f) Pinnate vein systems linked by a through-going fracture may be (e) planar or (f) sigmoidal. Linked sigmoidal veins (f) comprise tips, curved parts and linked parts.

Durney and Ramsay (1973) emphasized the importance of mass-transfer processes, which are independent of fluid flow, in the formation of isolated veins. Such mass-transfer, in the presence of fluid, can occur along intercrystalline pathways. However, some vein textures record internal permeability paths resulting from incomplete sealing after fracture events (Laubach, 1988). In particular, it has been proposed that isolated quartz fibres can grow in contact with fracture walls while surrounded by fluid-filled cavities (Henderson et al., 1990). Fisher and Brantley (1992) proposed that disrupted crack-seal vein textures represented collapse resulting from fluid pressure drop. Such a process implies incomplete vein filling to allow room for a disruptive collapse to occur. The textures of sigmoidal veins have been studied with regard to vein filling textures; for example the coarsest quartz in the thick central parts of gently sigmoidal veins in sandstone was interpreted to indicate the effects of competition between adjacent crystals in a cavity (Nicholson, 1991).

Intracrystalline deformation of vein filling minerals is typically interpreted as being imposed on veins after their formation is complete. The deformation behaviour of quartz has been studied in detail; for example, Carter et al. (1964) experimentally reproduced some natural deformation features of quartz which they related to crystallography: namely, to the *c*-axis and basal plane. In a companion paper, Christie et al. (1964, p. 752) found that in compression normal to the *c*-axis "lamellae and conjugate kink bands develop at inclinations of approximately 45° to the *c*-axis". In naturally deformed rocks similar features have been classified as extinction bands, deformation bands and deformation lamellae (Vernon, 1976; Passchier and Trouw, 1996).

Vein quartz deformed by compression parallel to the basal [0001] plane under greenschist conditions can develop features such as 65–180-μm-wide deformed zones which Nishikawa and Takeshita (2000) referred to as kink bands. Within these kink bands the *c*-axis is rotated by 18–46° and the quartz is recrystallized, resulting in development of a so-called 'chess-board' extinction pattern due to the presence of conjugate kinks. van Daalen et al. (1999) also investigated localized greenschist facies deformation in quartz vein fibres. They observed zones of deformation similar to those described above, but narrower, which they referred to as shear bands. They observed that the apparent shear sense of shear bands is consistent with offsets recognised from grain boundary offsets or mutual offsets of shear bands. These conjugate shear bands were found to be more common in fibres with *c*-axes along the length of fibres. They interpreted this to be a consequence of shear deformation (initiated by brittle microfaults) parallel to the crystallographic rhomb faces. Within shear bands, quartz is recrystallised such that *c*-axes are sub-parallel with shear band boundaries (when compression is at a high angle to host crystal *c*-axis) or *c*-axes are at a high angle to the shear band margins (where *c*-axis of the host crystal is parallel to compression). They also observed fragments of the host grain that had been detached and rotated during the formation of the shear bands. Orientation of the conjugate kink/shear bands is crystallographically controlled, approximately parallel to the *r*- and *z*-rhomb planes and the magnitude of deformation in individual quartz grains is controlled by their orientation with respect to applied stress axes (Neumann, 2000). Casas (1986) recognized conjugate shear bands similar to those described above except that they hosted en échelon arrays of microcracks. The microstructures occur in a quartz mylonite and Casas (1986) interpreted them as early brittle features instrumental in the progressive grain-size reduction of the mylonite.

This paper describes textures in quartz vein samples representative of various stages of deformation contemporaneous with vein filling. The synkinematic vein textures record a complex interplay between opening of new fractures or grain boundaries and sealing by mineral deposition and apparently ductile deformation such as the formation of deformation bands. The textures reveal the transient porosity and inferred fluid pathways through the veins during their development. Advances in hydraulic modelling of vein systems will be reliant on realistic interpretations of vein microstructures.

## 2. Geological setting

The Boyd Volcanic Complex, exposed in the northern and central parts of the field area (Fig. 1), comprises diverse, mainly terrestrial, facies of felsic to mafic composition ranging in thickness up to 1500 m (Fergusson et al., 1979; Cas et al., 1990). Overlying the volcanics are Late Devonian

Table 1
Vein microstructures described and their presence (tick) or absence (cross) in sampled vein systems

| | Host rock | Volcanic | | | | | Sandstone | | | | | | | | | | | | | |
|---|---|---|---|---|---|---|---|---|---|---|---|---|---|---|---|---|---|---|---|---|
| | Vein morphology | Planar | | | | | Planar | | | | | | | | Curved | | | Linked | | |
| | Sample | TT | TG | LO | BH | AB | TR | SH | HA | LE | WO | GR | NM | SM2 | SL | BI | SM1 | BA | RE | SA |
| | Vein width (mm) | 6 | 10 | 4 | 5 | 11 | 3 | 13 | 8 | 9+ | 5 | 17 | 30 | 5 | 50+ | 25+ | 50+ | 50+ | 50+ | 20 |
| Structures | Interpreted process | Occurrences | | | | | | | | | | | | | | | | | | |
| Cloudy fibrous quartz | Synkinematic growth | ✓ | ✓ | ✓ | ✓ | ✓ | ✓ | ✓ | ✓ | ✓ | ✓ | ✓ | ✓ | ✓ | ✓ | ✓ | ✓ | ✓ | ✓ | ✓ |
| En échelon microcracks in zones of extinction angle misorientation (Fig. 9c and d) | Brittle microcrack arrays formed in compression | ✓ | ✓ | ✓ | ✓ | × | ✓ | × | × | × | × | ✓ | × | × | ✓ | × | × | ✓ | × | ✓ |
| Curved fibres with undulose extinction (Fig. 9e) | Bending/buckling/kinking of fibres | × | × | × | × | × | × | × | × | ✓ | × | ✓ | × | × | ✓ | × | ✓ | ✓ | ✓ | × |
| Clear blocky quartz | Cavity growth | ✓ | ✓ | ✓ | ✓ | ✓ | ✓ | ✓ | ✓ | ✓ | ✓ | ✓ | ✓ | ✓ | ✓ | ✓ | ✓ | ✓ | ✓ | ✓ |
| Transgranular clear zones (Fig. 9f) | Cross-cutting fractures | × | × | × | × | ✓ | × | ✓ | × | ✓ | ✓ | ✓ | ✓ | × | ✓ | ✓ | ✓ | ✓ | ✓ | × |
| Intergranular clear zones (Fig. 9g) | Grain boundary dilation | ✓ | ✓ | ✓ | ✓ | ✓ | ✓ | ✓ | ✓ | ✓ | ✓ | ✓ | ✓ | ✓ | ✓ | ✓ | ✓ | ✓ | ✓ | ✓ |
| Clear blocky quartz with euhedral terminations around cavities (all surrounded by fibrous cloudy quartz) (Fig. 9i and j) | Cavity growth in spaces formed by dilation of vein texture | × | × | ✓ | ✓ | × | × | ✓ | ✓ | ✓ | ✓ | ✓ | ✓ | ✓ | × | ✓ | ✓ | ✓ | ✓ | ✓ |
| Clear blocky quartz bounded by micaceous seams (Fig. 9k) | Splitting of micaceous seams | × | × | × | × | × | × | × | × | × | × | × | × | × | × | × | × | ✓ | ✓ | × |
| Zones of blocky and fibrous quartz parallel to vein margins | Margin-parallel growth zones | × | ✓ | ✓ | ✓ | ✓ | × | × | × | × | ✓ | ✓ | × | × | × | × | × | × | × | ✓ |
| Zones of blocky and fibrous quartz parallel to fibres (Fig. 9h) | Complex growth zones including isolated fibres | ✓ | ✓ | ✓ | ✓ | ✓ | ✓ | ✓ | ✓ | ✓ | ✓ | ✓ | ✓ | ✓ | ✓ | ✓ | ✓ | ✓ | ✓ | ✓ |

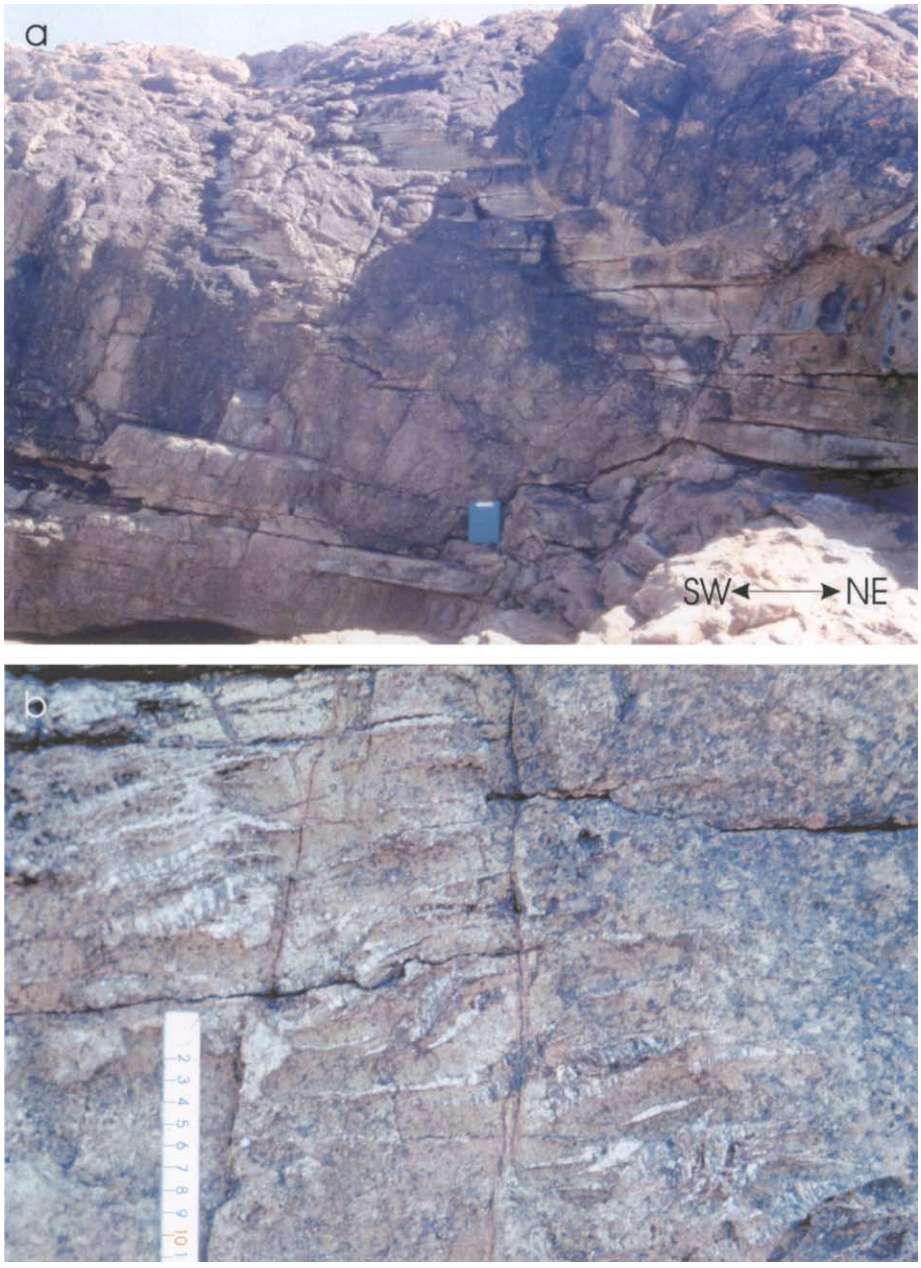


Fig. 3. (a) Field photograph of en échelon quartz vein arrays in columnar jointed rhyolite at Bunga Head (clipboard in lower centre is 24 cm wide). (b) Detail from (a) of a northwest over southeast array of sigmoidal quartz veins (tape measure is marked in centimetres).

fluvial and shallow marine sediments of the Merrimbula Group (locally subdivided), which comprise most of the coastal outcrops (Taylor and Mayer, 1990). The beds are commonly flat lying but locally folded and thrust faulted by east–west compression at a depth estimated at 1 km (Rixon et al., 1983). This eastern sub-province of the Lachlan Fold Belt was deformed by east–west compression in the Early Carboniferous, elsewhere accompanied by metamorphism up to greenschist facies (Gray, 1997).

Veins are present in the volcanic and sedimentary rocks and there is no indication that the rocks suffered significant deformation after the phase of vein formation. Coastal exposures of the Devonian sandstones of the Merrimbula Group, in particular, contain locally abundant vein arrays. Rickard and Rixon (1983) described the intimate relationship between quartz vein arrays and cleavage in the sandstone host rocks and concluded that the veins formed as ‘tension fractures’ (extension fractures) rather than shear fractures. The veins and vein arrays exploit the bedding and cross-bedding anisotropy of the sandstone host rocks. Smith (1999) described one locality (Fig. 1, SH) at which the arrays of veins form as incipient thrust faults. The occurrence of complex vein-filling processes is evidenced by Rickard and Rixon’s (1983, fig. 2c) observation of en échelon arrays of fracture-like cavities within a quartz vein. Correct interpretation of the formation and deformation of

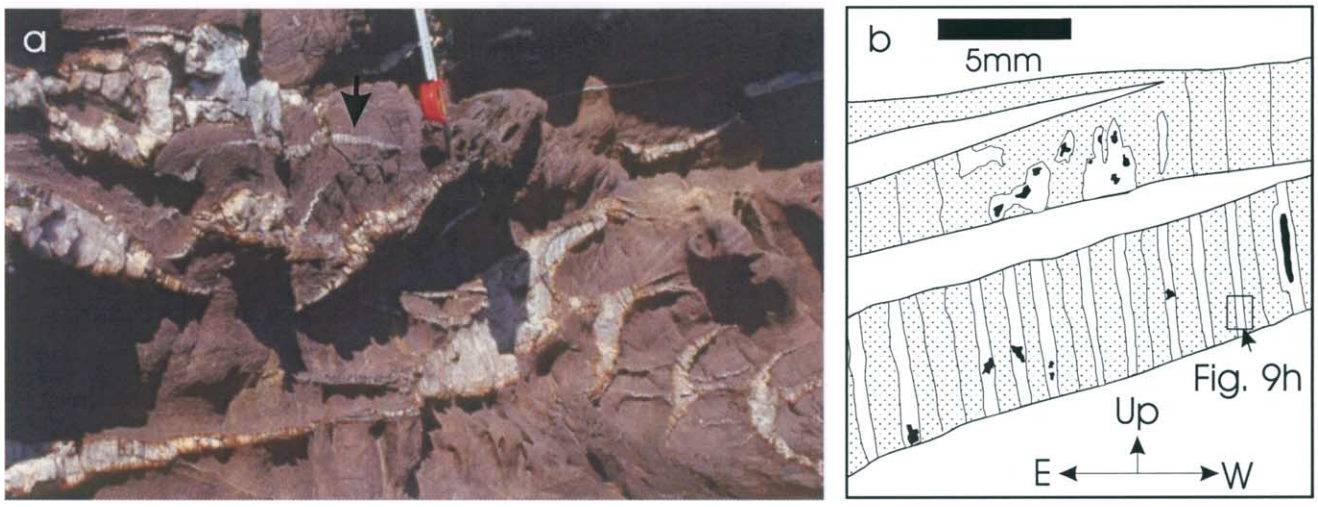


Fig. 4. (a) Field photograph of an en échelon vein array (non-profile exposure) at Short Point, Merimbula (Fig. 1; vein array 6 of Smith (1999)) (field of view 1.5 m across, arrow marks sample). (b) Line drawing from thin section of planar veins and sigmoidal vein tips (thin section is oriented parallel to the profile plane). Sandstone host veins comprising fibrous (stippled) and blocky (unstippled) quartz. Cavities (black) bounded by euhedral terminations occur within blocky quartz zones.

vein filling textures during synkinematic crystal growth is potentially a useful tool for investigating the history of fluid pressure variations and hydraulic fracturing at the depths represented in this region.

## 3. Vein array types and sampling

At 17 selected exposures along 70 km of coast from Bunga Head in the north to south of the Merrica River estuary, well-exposed vein systems were mapped, and oriented samples were collected. Three-dimensional structural analysis shows that most of the vein systems hosted by sedimentary rocks developed during horizontal to gently plunging northwest–southeast through to northeast–southwest contraction and near vertical extension (Fig. 1). An exception was noted at the Barmouth location (Fig. 1, BA) where veining occurs on a reverse fault parallel to locally steep dipping beds. The volcanic-hosted veins (Fig. 1, TT, TG, LO) recorded a range of stress orientations (relative to present coordinates).

The veins range in shape from planar to strongly sigmoidal, although those hosted by volcanic rock are rarely more than gently sigmoidal. Degrees of sigmoidality will be defined according to arbitrary geometric limits illustrated in Fig. 2a–d. However, this geometric parameter is commonly variable within an array in the dimension perpendicular to the profile (Nicholson, 1991; Smith, 1996) and along the array profile (Smith, 1999). Vein arrays range from those with discrete vein segments to those that have been linked by through-going faults to form pinnate vein systems. Pinnate veins commonly exhibit strongly sigmoidal, pre-cursor arrays; however, this is not always so as planar pinnate veins can occur, depending on the brittleness of the rock under the conditions of deformation (Fig. 2e and f).

Vein arrays are most simply viewed and photographed in planar exposures parallel to the profile plane, which is normal to both the veins and their host array. However, arrays with non-planar exposures are often overlooked but are actually more suitable for three-dimensional measurement and block sampling. Samples were taken from both photogenic and non-photogenic (non-planar) exposures. Samples were taken to represent types of veins and/or specific parts of veins, namely, planar vein tips, curved parts of sigmoidal veins and linked parts of pinnate veins (Fig. 2f; Table 1). Examples of planar vein parts are samples BH and SH which were obtained from the tips of gently to moderately sigmoidal veins in arrays hosted by rhyolite (Fig. 3) and sandstone (Fig. 4), respectively. An example of a curved vein part is sample SL (Fig. 5), which was obtained from an array of strongly sigmoidal pinnate veins. An example of a linked vein part is sample RE (Fig. 6), which was obtained from the central part of pinnate veining along a reverse fault. The range of en échelon vein types from planar through sigmoidal to veins linked by through-going faults are inferred to represent a sequence of cumulative deformation. Similarly, within individual veins, different stages of such a deformation sequence are recorded in each part of the vein system, that is, planar vein tips record the stage of fracture initiation and opening whether they are part of an array of planar, sigmoidal or linked veins.

On the headland south of the Saltwater Creek estuary (Fig. 1, SA), sub-planar veins with fibres at a low angle to the vein margins occur in open folded sandstone and mudstone interbeds (Fig. 7). The shear sense of the veins is indicated by the fibres and the low angle pinnate apophyses on the vein (Fig. 7c), both of which indicate a top-to-the-west movement. This structure is interpreted to have

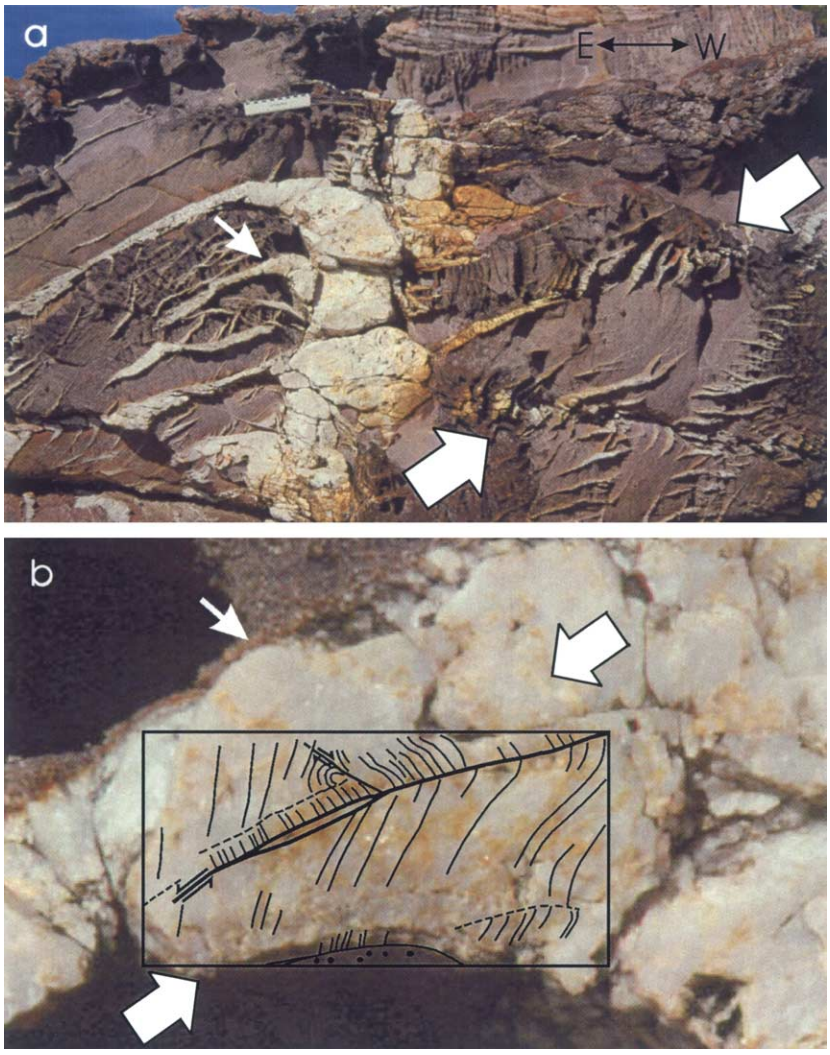


Fig. 5. (a) Field photograph of veins at a locality approximately 2 km south of Lennards Island (Fig. 1) (scale at top left of centre is 15 cm long). The major principal compressive stress axis (large arrows) bisects the conjugate vein systems. (b) Detailed field photograph (small arrows mark the same point in each image) with line drawing from thin section (superimposed) showing deformed quartz fibres including an isoclinal fold (centre), fault (thick line and thick shear arrows) and location of microscopic intragranular microcrack arrays (thin shear arrows). The kinematics of the fault and microcrack arrays is consistent with the inferred maximum principal compressive stress axis (large white arrows).

evolved as an early east-dipping thrust fault that was tilted to the west during folding. The interpretation is supported by fibre-parallel compression microstructures that will be described below. The open upright folds developed in bulk west over east shearing as evidenced by westward dipping cleavage and the rotation of clastic dykes relative to bedding on the west-dipping limb only (Fig. 7).

## 4. Vein microstructures

The veins are composed almost entirely of quartz with minor chalcedony and carbonate. Albite is a common component of the veins hosted by volcanic rock. The veins are commonly fibrous and range from having few to abundant cavities. The widths of the veins sampled vary and generally increase from planar through curved to linked veins (Table 1).

Two main petrographic types of quartz are recognized: fibrous to elongate quartz with abundant fluid inclusions that have a cloudy appearance (Fig. 8a) and blocky to polygonal quartz that is clear in appearance (Fig. 8b). Complex microstructures within the veins are composed of these two main textural elements.

### *4.1. Cloudy fibrous quartz*

Fibrous quartz with abundant fluid inclusions is observed to be common in all veins sampled (Table 1) Intergranular boundaries are typically irregular to columnar (Figs. 8c and 9a and b). Undulose extinction is present in most fibrous grains and is commonly localized along conjugate bands. At

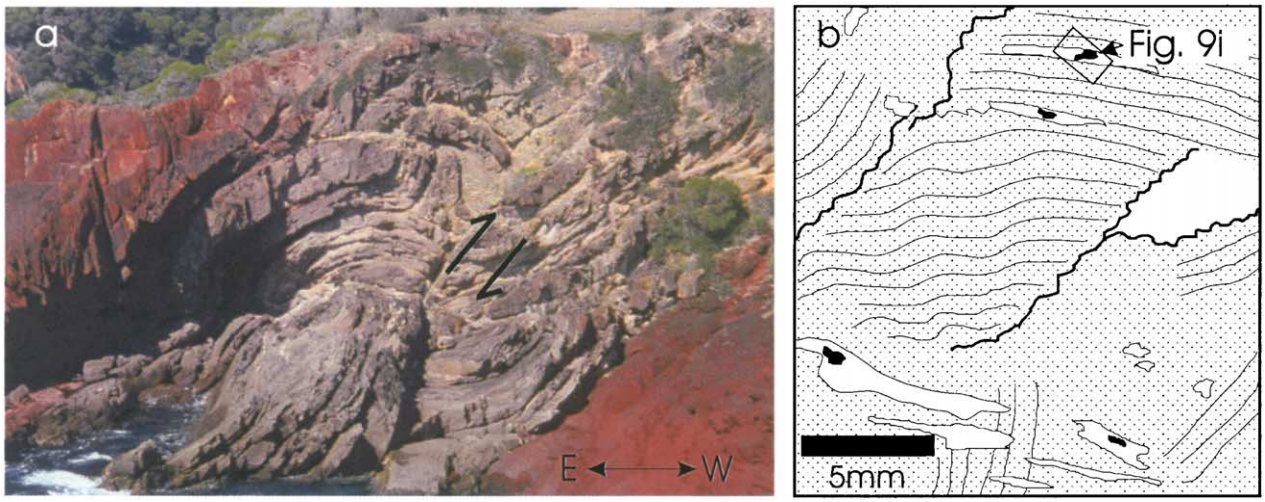


Fig. 6. (a) Field photograph of fold and thrust fault (shear arrows) at Red Point (Fig. 1). (b) Line drawing from thin section of a sample obtained from the linked en échelon quartz vein hosted by the thrust fault. Folded fibrous quartz (stippled) occurs in zones separated by micaceous seams. Blocky quartz (unstippled) occurs as elongate transgranular zones (bottom), fibre-parallel zones (top) and where a micaceous seam has been split (right). Cavities (black) bounded by euhedral terminations occur in many of the blocky quartz zones.

low magnification (Figs. 8d and 9c) these microstructures appear similar to other deformation microstructures in quartz (e.g. van Daalen et al., 1999; Nishikawa and Takeshita, 2000). High magnification reveals that en échelon arrays of microcracks occur along each zone of lattice misorientation (Figs. 8e and 9d) within crystals similar to those described by Casas (1986). The misorientation can locally be resolved into individual rotated blocks between microcracks, a geometry typical of brittle failure (Bazant and Xiang, 1997). The deformation microstructures have a typical width of approximately 10 μm (9.8 μm with standard deviation 3.7 μm for $n=56$) and spacing between bands varies from 30 to 100 μm. The misorientation of the lattice between shear bands and host crystal is approximately 8° (7.8° with standard deviation 5.1° for $n=56$) with a sense of rotation consistent with the sense of shear on the band. The lattice misorientation is thus inferred to be a consequence of the rotation of the bridges between microcracks.

In most examples, both left-handed and right-handed shear bands are present as conjugate pairs. The conjugate shear bands and their arrays of microcracks have reflectional symmetry of lattice deflection across the bisecting plane. The microcracks are generally oriented approximately parallel to the bisector of conjugate arrays although some examples have convergent fracture array geometries (Smith, 1996). The conjugate angles are consistently less than 90°, being 66° on average (with standard deviation 15° for $n=28$). The compression direction inferred from the bisector of conjugate microcrack arrays is most commonly oriented at either high or low angles to the *c*-axis of the host crystal (Fig. 10). This observation is similar to that observed in (supposedly) non-brittle deformation bands in quartz (van Daalen et al., 1999; Nishikawa and Takeshita, 2000) further supporting a close relationship between these types of microstructures.

Quartz fibres locally exhibit curvature and undulose extinction indicative of bending after initial crystallisation. In an extreme example, isoclinally folded quartz fibres were observed (Fig. 9e). Concentrations of insoluble material occur in samples from linked parts of veins.

### 4.2. Clear blocky quartz

Clear blocky quartz is commonly associated with the fibrous quartz representing up to about 50% of the filling of most vein types Cross-cutting microveins, typically extending beyond individual grain boundaries, are a common feature (Fig. 9f). The overprinting relationship of the microveins indicates that the clear blocky quartz is younger than the cloudy fibrous quartz in that setting.

Other petrographic relationships include clear blocky quartz along grain boundaries. In these situations an angular or zig-zag shaped grain boundary is flanked by zones of clear quartz in optical continuity with cloudy fibrous quartz (Figs. 8f and 9g). Clear blocky quartz also forms in zones parallel to cloudy quartz fibres (Figs. 8g and 9h). Cavities were observed in some veins, typically lined with clear blocky quartz with euhedral terminations in the cavities (Fig. 8h). In some cases these cavities form strings parallel to quartz fibres (Fig. 9i and j).

Where wall-rock seams are present, patches of clear quartz are typically associated. In some cases, wall-rock seams bifurcate and clear quartz is located between the parts of the seam (Figs. 8i and 9k).

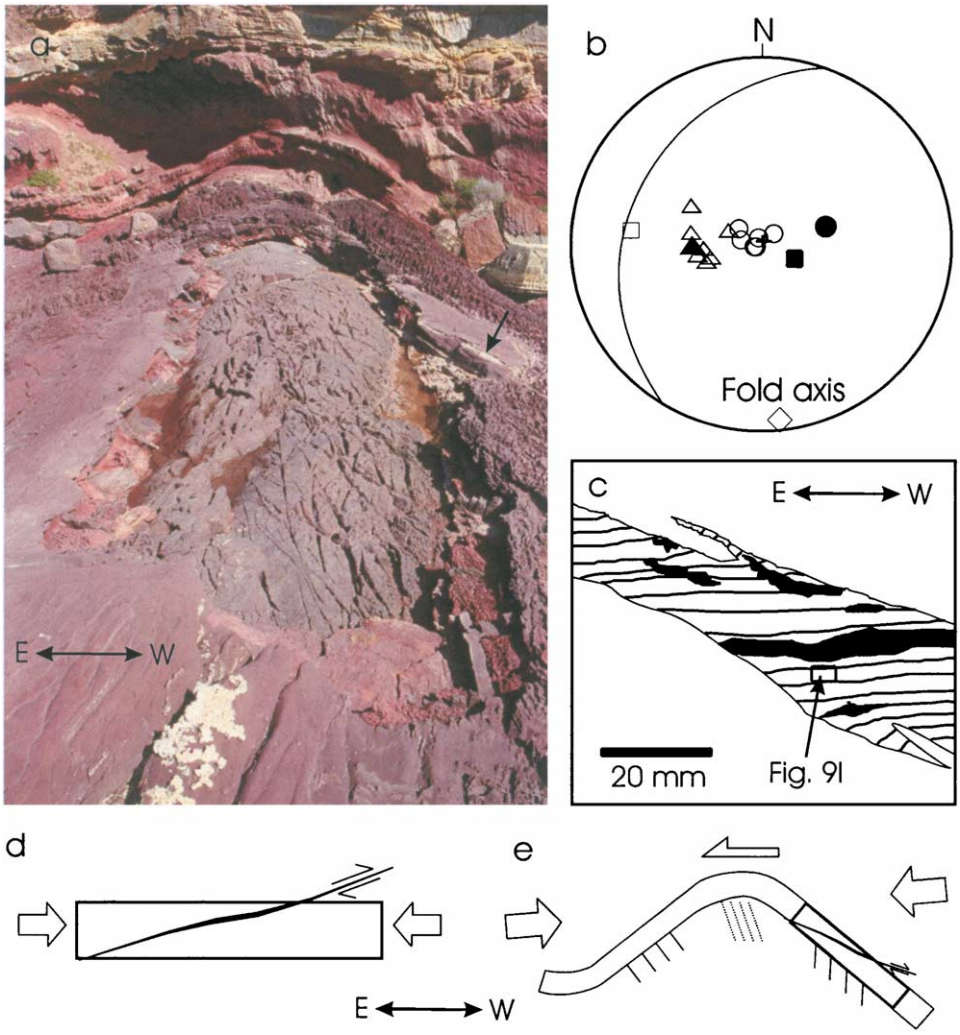


Fig. 7. (a) Field photograph of an open upright anticline south of the Saltwater Creek estuary (Fig. 1). West-dipping cleavage can be seen at the top. Sand dykes are exposed on each limb of the fold. (b) Stereogram (equal angle) showing vein (solid square pole and great circle) with shear fibre traces (open square), poles to bedding on fold limbs (solid circle and triangle) and lines of intersection of sand dykes (open symbols same shape as host limb symbols). The east-dipping limb has perpendicular clastic dykes whereas on the west-dipping limb clastic dykes are tilted with respect to bedding recording overall west-over-east shearing. (c) Detail of mainly fibrous quartz (lines) and cavities (black) in a brittle pinnate shear vein. (d) and (e) The shear vein is interpreted to have formed during bedding-parallel compression by east-over-west thrusting followed by rotation of the bed which induced fibre-parallel compression structures.

## 5. Vein textures and vein morphology

### 5.1. Textures in planar veins and vein tips

In planar veins and the planar tips of other vein types, the vein-filling textures do not show signs of intense deformation present in curved and linked vein parts. However, intragranular undulose extinction and associated microcrack arrays occur in many of the planar veins. Typically, both cloudy fibrous and clear blocky petrographic types of quartz are present. The most commonly observed textural relationship is zones of clear quartz parallel to fibres. This texture was found to be more common than margin-parallel zoning (Table 1). Intergranular clear zones are also commonly present, as are cavities with clear quartz linings.

### 5.2. Textures in sigmoidal curved veins

The sigmoidal curvature of veins is accompanied by the formation of microstructures including dilated grain boundaries and through-going microfractures. Complex intergrowths of cloudy fibrous quartz and clear blocky quartz and local cavities lined with euhedral quartz record the complex pattern of intra- and intercrystalline deformation. Where present, microcrack arrays show that the deformation of the vein textures proceeded under a steady vein tip-parallel contraction.

### 5.3. Textures in linked veins

Linked veins represent areas where vein arrays have developed into through-going faults or where sigmoidal

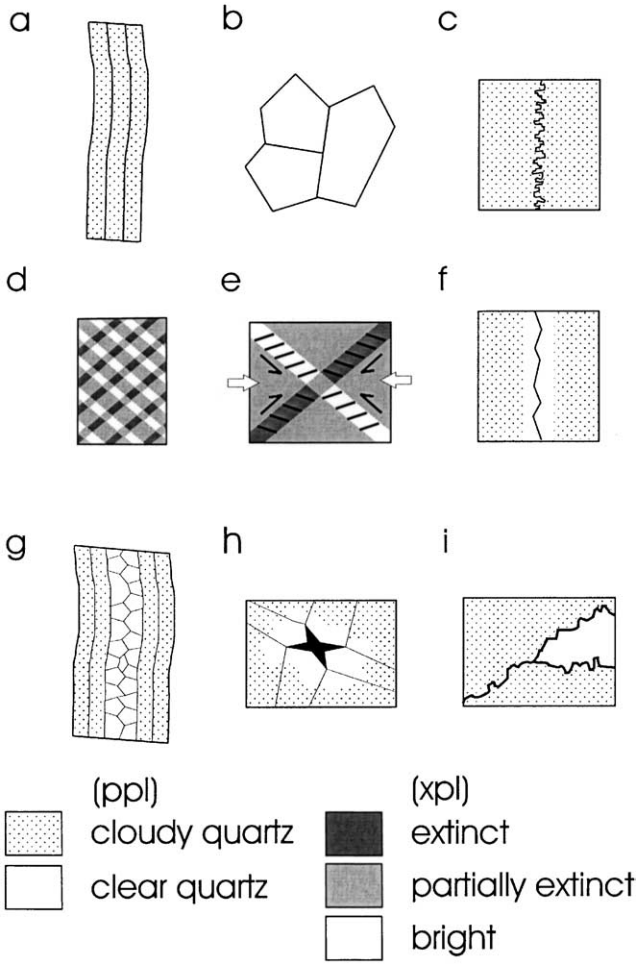


Fig. 8. Schematic illustration summarizing vein microstructures described in the text. (a) Cloudy fibrous quartz grains. (b) Clear blocky quartz grains. (c) Irregular quartz–quartz grain boundary. (d) Conjugate deformation bands in quartz producing a 'tartan' appearance under cross polarized light. (e) Detail of (d) showing the presence of microcracks and senses of shear. (f) Quartz–quartz grain boundary with a clear quartz zone and apparent intergrowth texture. (g) Fibres of cloudy quartz with parallel zones containing clear blocky quartz. (h) Cavity (black) bounded by euhedral terminations of clear blocky quartz (unstippled) surrounded by fibrous quartz (stippled). (i) Clear blocky quartz (unstippled) bounded by micaceous seams (heavy lines) which appear to have formed by the splitting of a single seam.

veins have merged by progressive dissolution of wall-rock bridges. The degree of sigmoidal curvature toward the vein tips is an indication of the extent of ductile deformation involved in the linking of the veins. The vein systems sampled show at least some sigmoidal curvature. In strongly sigmoidal linked vein systems, micaceous seams develop from the wall-rock bridges that separated vein segments. The spacing between seams is approximately similar to the width of individual veins projecting from the central part of the vein system showing that they formed by merging of the veins.

Linked vein textures typically comprise blocks of fibrous quartz separated by microfaults or zones of clear blocky quartz and cavities lined with euhedral quartz. The zones of clear quartz record disruption of the fibrous quartz in-filling during on-going deformation including transgranular microcracks, dilation of grain boundaries and splitting along weak micaceous seams. The infilling is effectively a quartz-in-quartz microbreccia.

## 6. Discussion

### 6.1. Porosity textures

The textures of the linked vein samples reveal evidence of shear-related dilation of the vein rock by a combination of transgranular and intragranular microfracturing, microfaulting and parting of grain boundaries and micaceous seams. The latter stages of infilling are recognized by the presence of cavities surrounded by clear blocky quartz. This process would involve cyclic deformation analogous to crack-seal veins (Ramsay, 1980a) but with a brecciated pattern rather than regular margin-parallel microstructures. However, associations of clear blocky quartz and cloudy fibrous quartz are also common in vein tips and planar veins. In these cases the absence of evidence of significant distortion of the fibrous grains indicates that the fibres grew in the presence of abundant porosity between fibres or groups of fibres. These spaces were later infilled or partly infilled by clear quartz.

### 6.2. Conjugate microcrack arrays

The microcrack arrays are found both in low strain (planar veins and vein tips) and high strain (sigmoidally curved veins and linked veins) settings The study of fracture arrays has historically concentrated on the question of cause and effect, that is, whether microcrack arrays are the product of strain in a shear zone or alternatively if pervasive parallel cracks become locally intensified to form a zone of shear displacement. Beach (1975) proposed Type I and Type II vein arrays as forming by these processes, respectively. The argument has centred on timing and cause and effect relationships between fractures and their host zones and has important implications for the nature of deformation mechanisms. A method of testing the hypotheses is use of the concept illustrated by Ramsay (1980b) that the angle between conjugate shear zones is related to the dilatancy (that is, dilation associated with shearing) occurring in the deformation zones at the time of their initiation. Shear zones that initiate without change in volume produce conjugate angles of 90°, indicating zero dilatancy. If brittle fractures subsequently form this will not alter the angle between conjugate shear zones. If brittle fractures exist prior to, and/or during the initiation of, the shear zones then conjugate angles less than 90° will reflect the dilatancy of the fracturing. These observations need to be tempered by the possibility that superposed deformation may result in

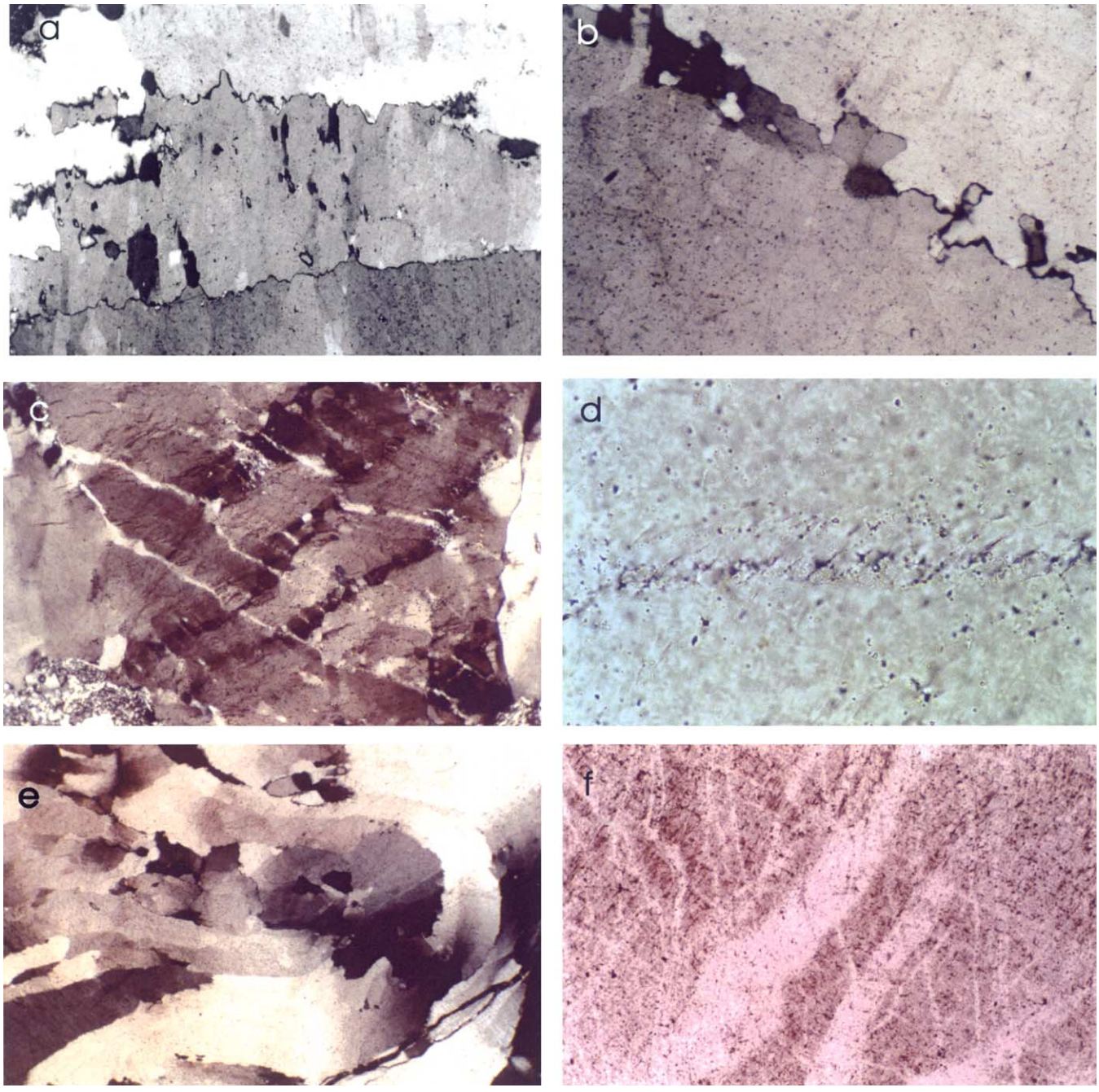


Fig. 9. Photomicrographs. (a) Quartz fibres (horizontal) with irregular boundaries (field of view 3 mm; cross polarized light). (b) Irregular boundaries between quartz fibres (sample: SL; field of view 1.2 mm; cross polarized light). (c) Quartz strongly affected by crystallographic distortion by conjugate intragranular microcrack arrays (sample: TT; field of view 3 mm; cross polarized light). (d) Intragranular microcrack arrays (sample: TT; field of view 70 μm; plane polarized light). (e) Isoclinally folded quartz fibres (note bent extinction, sample: SL; field of view 3 mm; cross polarized light). (f) Clear quartz as zones cross-cutting cloudy quartz (field of view 1.2 mm; plane polarized light). (g) Intergranular clear zone adjacent to an angular intergrown boundary of quartz fibres (sample: SM1; field of view 1.2 mm; plane polarized light). (h) Fibre-parallel zone of equant grains of clear quartz adjacent to fibrous quartz (sample: SH; field of view 3 mm; cross polarized light). (i) Fibre-parallel cavities (top right to bottom left) lined with euhedrally terminating equant clear quartz (sample: RE; field of view 3 mm; partial cross polarized light). (j) Detail from the top right corner of (i). (k) Clear quartz along a micaceous seam interpreted as infill of an opening along the weak seam. (l) Fibrous quartz (fibres horizontal) with micro-shear bands with right-handed rotation (bright bands top left to bottom right) and left-handed rotation (dark bands bottom left to top right) indicating compression parallel to fibres (sample: SA; field of view 1 mm; cross polarized light).

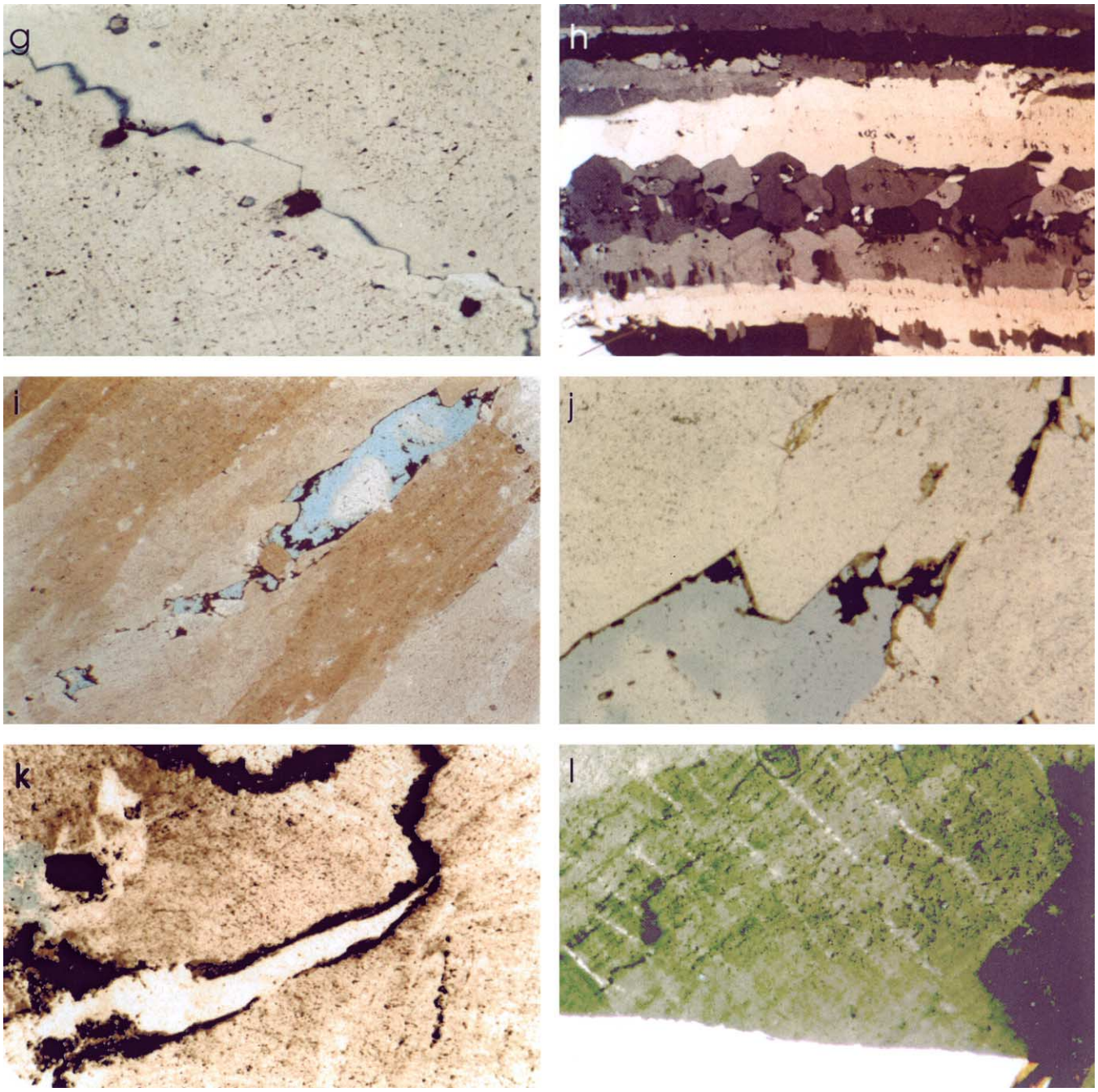


Fig. 9 (*continued*)

flattening and thus an increase in the dihedral angle. In this study dihedral angles between conjugate microshear zones are consistently less than 90°, indicating that dilatancy, i.e. microfracturing, existed during the initiation of the shear zones (deformation bands).

Previous work on conjugate intragranular deformation bands in quartz, such as van Daalen et al.'s (1999, fig. 5A–D) stereographic illustrations, show average conjugate angles between microshear zones of approximately 77, 95, 103 and 108°. Nishikawa and Takeshita's (2000) two-dimensional representations show conjugate angles of 62, 81 (their fig 2b) and 82° (their fig 3a). This sampling indicates diverse values but is too limited to attempt to interpret the possible role of microcracks in the development of the structures in these studies. Casas (1986) observed an angle between conjugate microcrack arrays of 80° but described a progressive increase in the angle up to 110° with increasing ductile strain in the mylonite.

The model for the deformation bands with microcrack arrays observed in quartz in this study is that pervasive microcracks began to form in a grain of quartz, then deformation became localised as en échelon fracture arrays

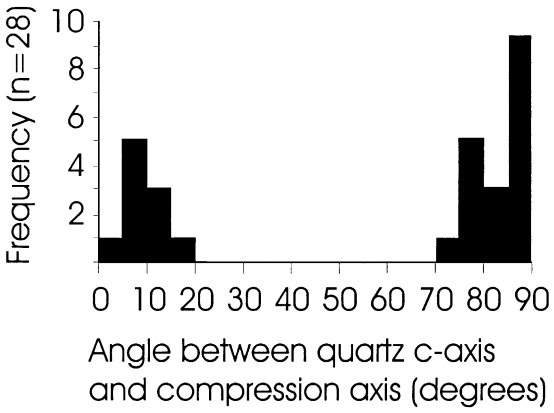


Fig. 10. Frequency histogram showing general parallel/orthogonal relationship between the compression axes determined from conjugate microcrack arrays and the *c*-axis of host quartz grains.

which opened by the bending of the thin bridges between fractures. The arrays may be open to fluids from grain boundaries but infilling would stop when the fractures became isolated. Arrays of linked microcracks were not observed, which indicates either a limit to the deformation or that linked microcracks become completely sealed by quartz and, thus, invisible.

For the volcanic-hosted veins the relationship between microcrack arrays, vein fibres and veins is relatively simple. In each example, fibres are approximately perpendicular to vein margins and the compression direction determined from microcrack arrays is perpendicular to fibres. Since microcracks are only present in fibres with crystallographic axes parallel to the length of the fibre, it is inferred that the microcracks developed due to the same compression responsible for the opening of the veins themselves. If the microcracks were simply the result of an arbitrary deformation(s) imposed on the vein, such a correlation between inferred compression directions of veins and intragranular microcracks would be unexpected.

For the planar sandstone-hosted veins (TR, GR), the relationship between veins, fibres and microcracks is the same as that described for the volcanic-hosted veins. For the curved vein containing microcrack arrays (SL), the compression direction is parallel to vein tips but the fibres hosting microcrack arrays have been rotated within the sigmoidal vein such that compression is parallel to the length of the fibres. For the linked vein with microcracks (BA), compression inferred from microcracks is parallel to vein tips, but fibre orientations were disrupted and the only fibres observed with microcrack arrays are perpendicular to the inferred compression axis. The brittle pinnate vein array linked into a shear vein (SA) has microcrack arrays recording sub-horizontal fibre-parallel compression (Fig. 9l). The fibres in this vein are relatively straight and it is inferred that, when the fold limb rotated, the vein was compressed parallel to the length of fibres. The vein is notable for its high porosity comprising abundant margin-parallel and fibre-parallel cavities that may have formed from brittle failure.

## 7. Conclusion

Quartz veins in Devonian sandstone and felsic volcanic rocks of South Coast, New South Wales contain microstructures indicating that crystal growth occurred in a wide variety of locations within the vein texture. A survey of veins shows that transgranular, intergranular and intragranular dilation provided abundant, mostly transient, pathways for dissolved material to be transported to internal growth sites in veins. The deformational microstructures of vein filling minerals, such as microcrack arrays superficially similar in appearance to deformation bands and lamellae, were found to be consistent with the kinematics of the vein opening. These observations are the necessary foundation to future determinations of appropriate hydraulic parameters such as aperture size and shape, and opening duration of natural fracture systems in rock.

## Acknowledgements

David Durney and Donald Fisher provided critical reviews of the paper. This project was funded by the Australian Research Council (grant A39906174).

## References

Bazant, Z.P., Xiang, Y., 1997. Size effect in compression fracture: splitting crack band propagation. Journal of Engineering Mechanics 123, 162–172.

Beach, A., 1975. The geometry of en-echelon vein arrays. Tectonophysics 28, 245–263.

Brantley, S.L., Fisher, D.M., Deines, P., Clark, M.B., Myers, G., 1997. Segregation veins: evidence for the deformation and dewatering of a low-grade metapelite, in: Holness, M.B. (Ed.), Deformation-Enhanced Fluid Transport in the Earth's Crust and Mantle. Chapman and Hall, London, pp. 267–288.

Carter, N.L., Christie, J.M., Griggs, D.T., 1964. Experimental deformation and recrystallization of quartz. Journal of Geology 72, 687–733.

Cas, R.A.F., Allen, R.L., Bull, S.W., Clifford, B.A., Wright, J.V., 1990. Subaqueous rhyolitic dome-top tuff cones: a model based on the Devonian Bunga Beds, southeastern Australia and a modern analogue. Bulletin of Volcanology 52, 159–174.

Casas, J.-M., 1986. Shear bands and related extensional structures in a mylonitized quartz dyke. Journal of Structural Geology 8, 693–699.

Christie, J.M., Griggs, D.T., Carter, N.L., 1964. Experimental evidence of basal slip in quartz. Journal of Geology 72, 734–756.

Cox, S.F., 1999. Deformational controls on the dynamics of fluid flow in mesothermal gold systems, in: McCaffrey, K., Lonergan, L., Wilkinson, J. (Eds.), Fractures, Fluid Flow and Mineralization Geological Society of London Special Publication, 155, pp. 123–140.

Durney, D.W., Ramsay, J.G., 1973. Incremental strains measured by syntectonic crystal growth, in: de Jong, K.A., Scholten, R. (Eds.), Gravity Tectonics. Wiley, New York, pp. 67–96.

Fergusson, C.L., Cas, R.A.F., Collins, W.J., Craig, G.Y., Crook, K.A.W.,

Powell, C.McA., Stott, P.A., Young, G.C., 1979. The Late Devonian Boyd Volcanic Complex, Eden, N.S.W.: a reinterpretation. Geological Society of Australia Journal 26, 87–105.

Fisher, D.M., Brantley, S.L., 1992. Models of quartz overgrowth and vein formation: deformation and episodic fluid flow in an ancient subduction zone. Journal of Geophysical Research 97, 20,043–20,061.

Gray, D.R., 1997. Tectonics of the southeastern Australian Lachlan Fold Belt: structural and thermal aspects, in: Burg, J.-P., Ford, M. (Eds.), Orogeny Through Time Geological Society of London Special Publication, 121, pp. 149–177.

Gray, D.R., Gregory, R.T., Durney, D.W., 1991. Rock-buffered fluid-rock interaction in deformed quartz-rich turbidite sequences, eastern Australia. Journal of Geophysical Research 96, 19,681–19,704.

Henderson, J.R., Henderson, M.N., Wright, T.O., 1990. Water-sill hypothesis for the origin of certain veins in the Meguma Group, Nova Scotia, Canada. Geology 18, 654–657.

Laubach, S.E., 1988. Subsurface fractures and their relationship to stress history in East Texas basin sandstone. Tectonophysics 156, 37–49.

Lewis, P.C., Glen, R.A., Pratt, G.W., Clarke, I., 1994. Bega-Mallacoota 1:250,000 geological sheet SJ/55-4, SJ/55-8: Explanatory Notes. Geological Survey of New South Wales, Sydney.

Means, W.D., Li, T., 2001. A laboratory simulation of fibrous veins: some first observations. Journal of Structural Geology 23, 857–863.

Neumann, B., 2000. Texture development of recrystallised quartz polycrystals unravelled by orientation and misorientation characteristics. Journal of Structural Geology 22, 1695–1711.

Nicholson, R., 1991. Vein morphology, host rock deformation and the origins of the fabrics of echelon mineral veins. Journal of Structural Geology 13, 635–641.

Nicholson, R., Pollard, D.D., 1985. Dilation and linkage of echelon cracks. Journal of Structural Geology 7, 583–590.

Nishikawa, O., Takeshita, T., 2000. Progressive lattice misorientation and microstructural development in quartz veins deformed under subgreenschist conditions. Journal of Structural Geology 22, 259–276.

Passchier, C.W., Trouw, R.A.J., 1996. Microtectonics. Springer, Berlin.

Ramsay, J.G., 1980a. The crack-seal mechanism of rock deformation. Nature 284, 135–139.

Ramsay, J.G., 1980b. Rock ductility and its influence on the development of tectonic structures in mountain belts, in: Hsu, K.J. (Ed.), Mountain Building Processes. Academic Press, London, pp. 111–127.

Rickard, M.J., Rixon, L.K., 1983. Stress configurations in conjugate quartz vein arrays. Journal of Structural Geology 5, 573–578.

Rixon, L.K., Bucknell, W.R., Rickard, M.J., 1983. Megakink folds and related structures in the Upper Devonian Merrimbula Group, South Coast New South Wales. Geological Society of Australia, Journal 30, 277–293.

Smith, J.V., 1996. Geometry and kinematics of convergent vein array systems. Journal of Structural Geology 18, 1291–1300.

Smith, J.V., 1999. Inter-array and intra-array kinematics of en echelon sigmoidal veins in cross-bedded sandstone, Merimbula, southeastern Australia. Journal of Structural Geology 21, 387–397.

Taylor, G., Mayer, W., 1990. Depositional environments and palaeogeography of the Worange Point Formation, New South Wales. Australian Journal of Earth Sciences 37, 227–239.

van Daalen, M., Heilbronner, R., Kunze, K., 1999. Orientation analysis of localized shear deformation in quartz fibres at the brittle–ductile transition. Tectonophysics 303, 83–107.

Vernon, R.H., 1976. Metamorphic Processes. George Allen and Unwin, London.